Structures and Magnetic Properties of Some Fe(III) Complexes with Hexadentate Ligands: in Connection with Spin-Crossover Behavior

Shinya Hayami,* Takashi Matoba, Shuichi Nomiyama, Takahiko Kojima, Susumu Osaki,† and Yonezo Maeda

Department of Chemistry, Faculty of Science, Kyushu University, Hakozaki, Higashi-ku, Fukuoka 812-81

†Radioisotope Center, Kyushu University, Hakozaki, Higashi-ku, Fukuoka 812-81

(Received May 2, 1997)

Several iron(III) complexes with the different hexadentate Schiff-base ligands of N_4O_2 donor sets were synthesized; these are 1 : 2 condensation products of linear tetramines (3,3,3-, 3,2,3-, 2,3,2- or 2,2,2-tetramine) and salicylaldehyde, acetophenone or benzophenone derivatives. Their crystal structures, Mössbauer spectra, magnetic susceptibilities, electronic spectra and cyclic voltammetry of the complexes were examined. The X-ray structures of the single crystals of [Fe(3,2,3-sal$_2$tet)]NO_3 (**1**), [Fe(3,2,3-sal$_2$tet)]BPh_4 (**2**), [Fe(3,2,3-mpk$_2$tet)]PF_6 (**3**), [Fe(2,3,2-sal$_2$tet)]ClO_4 (**4**), [Fe(2,3,2-3MeO-sal$_2$tet)]ClO_4 (**5**), [Fe(2,3,2-mpk$_2$tet)]ClO_4 (**6**), [Fe(2,3,2-bpk$_2$tet)]ClO_4 (**7**), and [Fe(2,2,2-bpk$_2$tet)]ClO_4·EtOH (**8**) were determined. Crystal data for (1): $C_{22}H_{28}N_5O_5Fe$, space group $P2_1/c$, $Z=4$, $a=7.607(1)$, $b=16.063(1)$, $c=19.063(1)$ Å, $\beta=91.00(2)°$, $V=2329(3)$ Å^3, $R=5.8\%$, $R_w=4.2\%$, 4605 reflections. Crystal data for (2): $C_{46}H_{48}N_4O_2BFe$, space group $P2_1/n$, $Z=4$, $a=14.390(6)$, $b=20.617(8)$, $c=14.754(5)$ Å, $\beta=115.85(2)°$, $V=3939(2)$ Å^3, $R=6.3\%$, $R_w=6.7\%$, 7458 reflections. Crystal data for (**3**): $C_{24}H_{32}N_4O_2PF_6Fe$, space group $P2_1/c$, $Z=4$, $a=9.37(6)$, $b=24.15(7)$, $c=12.85(3)$ Å, $\beta=97.7(3)°$, $V=2880(17)$ Å^3, $R=10.9\%$, $R_w=13.6\%$, 5569 reflections. Crystal data for (4): $C_{21}H_{26}N_4O_6ClFe$, space group $Pbcn$, $Z=4$, $a=11.041(2)$, $b=17.251(2)$, $c=11.722(2)$ Å, $V=2232(1)$ Å^3, $R=3.9\%$, $R_w=2.8\%$, 2258 reflections. Crystal data for (**5**): $C_{23}H_{30}N_4O_8ClFe$, space group $Pccn$, $Z=8$, $a=14.567(1)$, $b=22.288(1)$, $c=15.477(1)$ Å, $V=5025(4)$ Å^3, $R=6.3\%$, $R_w=6.2\%$, 4956 reflections. Crystal data for (**6**): $C_{23}H_{30}N_4O_6ClFe$, space group $Pbca$, $Z=8$, $a=28.249(4)$, $b=13.989(4)$, $c=13.174(4)$ Å, $V=5205(1)$ Å^3, $R=8.2\%$, $R_w=8.4\%$, 5148 reflections. Crystal data for (**7**): $C_{33}H_{34}N_4O_6ClFe$, space group $P\bar{1}$, $Z=2$, $a=10.241(3)$, $b=17.373(1)$, $c=9.692(7)$ Å, $\alpha=105.95(6)°$ $\beta=91.61(4)°$, $\gamma=93.83(4)°$, $V=1652(1)$ Å^3, $R=7.1\%$, $R_w=7.6\%$, 6179 reflections. Crystal data for (**8**): $C_{34}H_{38}N_4O_7ClFe$, space group $P2_1/c$, $Z=4$, $a=14.553(4)$, $b=14.079(4)$, $c=16.959(6)$ Å, $\beta=94.92(3)°$, $V=3461(1)$ Å^3, $R=8.4\%$, $R_w=7.7\%$, 6651 reflections. The moieties of the iron atoms of (**1**), (**2**), and (**3**) with 3,2,3-tetramine, and (**7**) with 2,3,2-tetramine were pseudo octahedral with *trans*-FeN_4O_2 geometry. Those of (**4**), (**5**), and (**6**) with 2,3,2-tetramine, and (**8**) with 2,2,2-tetramine were *cis*-FeN_4O_2 geometry. The iron(III) complexes (**1**), (**2**), (**3**), and (**7**) were in the low-spin state, and the iron(III) complexes (**4**), (**5**), (**6**), and (**8**) were in the high-spin state.

In the electronic spectra, the wave lengths of the LMCT bands for the low-spin complexes were longer than those for the high-spin complexes. The values of redox potentials for the low-spin states were suggested to be 0.12 V more negative than those for the high-spin states.

A number of spin-crossover iron(III) complexes have been prepared.[1] Reports have clarified that the magnetic behaviors of the spin-crossover complexes in solids are influenced by molecular packings, hydrogen bondings and so on.[2—4]

Although we have studied the magnetic properties of new iron(III) spin-crossover complexes for the past several years,[5] we have not yet succeeded in getting information about what design of ligands is suitable to prepare spin-crossover complexes. The structures and the magnetic properties of iron(III) complexes with the schiff-base ligands of 3,3,3-, 3,2,3-, or 2,2,2-tetramine derivatives have been reported,[6—12] but no iron(III) complexes with the 2,3,2 system are reported as far as we know. We prepared the iron(III) complexes with 3,3,3-, 3,2,3-, 2,3,2-, or 2,2,2-tetramine to get information about the structural effect of ligands on the magnetic behavior of the complexes. In this paper, the origins of differences in ligand field strength between them are discussed on the base of the structures of the iron(III) complexes with 3,3,3-, 3,2,3-, 2,3,2-, or 2,2,2-tetramine which form 6,6,6-, 6,5,6-, 5,6,5-, or 5,5,5-membered chelate rings, respectively. Ligand abbreviators used here are drawn in Scheme 1.

Wilson and co-workers have studied the magnetic properties of iron(III) complexes with hexadentate ligands in solid and solution, and the crystal structures of [Fe(2,2,2-sal$_2$tet)]-X.[6—10] The crystal structures of [Fe(2,2,2-sal$_2$tet)]Br·$2H_2O$ (low-spin), [Fe(2,2,2-sal$_2$tet)]BPh_4 (spin-crossover), and [Fe-(2,2,2-sal$_2$tet)]PF_6 (spin-crossover) have been determined by Nishida and co-workers.[12] They have commented that all of the 12 angles subtended at a metal atom by the adjacent

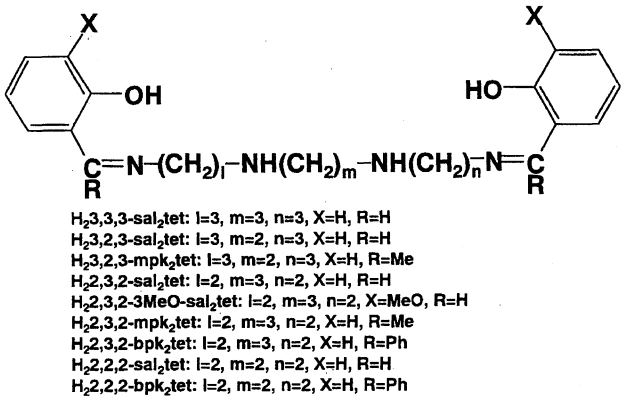

Scheme 1. Structures of the ligands.

atoms (N–Fe–N et al., which should be 90° in a regular octahedra) lie in the range from 75 to 105° for the spin-crossover complexes and from 84 to 95° for the low-spin complexes, and that all of the three angles L–Fe–L′ (*trans* position) are greatly deviated from 180° for the spin-crossover complexes and close to 180° for the low-spin complexes. The size effects of chelate rings on the spin states of [Fe(3,3,3-sal$_2$tet)]NO_3 (high-spin) and [Fe(3,2,3-sal$_2$tet)]$NO_3 \cdot H_2O$ (low-spin) have been discussed by Ito and co-workers.[11]

Experimental

Preparation of the Complexes. [Fe(2,3,2-sal$_2$tet)]ClO_4: $H_2$2,3,2-sal$_2$tet was prepared by adding *N*,*N*′-bis(2-aminoethyl)-1,3-propanediamine (0.32 g, 2 mmol) in methanol (20 ml) to a solution of salicylaldehyde (0.49 g, 4 mmol) in methanol (20 ml) under stirring. The solution turned yellow immediately; this was stirred at room temperature for 2 h. Then a solution of $Fe(ClO_4)_3 \cdot nH_2O$ (2 mmol) in methanol (20 ml) was added dropwise to the ligand solution, producing a dark purple solution. The solution was filtered and taken to dryness under reduced pressure at room temperature. The purple solid materials were recrystallized from an acetone–ethanol solution (approximately 1 : 1 by volume) by cooling with volume reduction under reduced pressure. The crystals were washed with ethanol, then ether, and dried under vacuum at room temperature over P_2O_5 for 4 h. Yield: 0.35 g, 36%. Other iron(III) complexes were prepared in a similar manner by use of appropriate tetramine and aldehyde, and the chemical compositions of the complexes were confirmed by elemental analysis. Microanalyses for carbon, hydrogen and nitrogen were carried out by the Elemental Analysis Center, Kyushu University. The data of the elemental analysis are listed below.

Anal. for [Fe(3,2,3-sal$_2$tet)]NO_3 (**1**). Calcd for $C_{22}H_{28}N_5O_5Fe$: C, 53.02; H, 5.66; N, 14.06%. Found: C, 52.51; H, 5.61; N, 13.90%. Anal. for [Fe(3,2,3-sal$_2$tet)]BPh_4 (**2**). Calcd for $C_{46}H_{48}N_4O_2BFe$: C, 73.12; H, 6.40; N, 7.42%. Found: C, 72.87; H, 6.54; N, 7.39%. Anal. for [Fe(3,2,3-mpk$_2$tet)]PF_6 (**3**). Calcd for $C_{24}H_{32}N_4O_2PF_6Fe$: C, 47.30; H, 5.29; N, 9.20%. Found: C, 47.43; H, 5.48; N, 9.07%. Anal. for [Fe(2,3,2-sal$_2$tet)]ClO_4 (**4**). Calcd for $C_{21}H_{26}N_4O_6ClFe$: C, 48.34; H, 5.02; N, 10.74%. Found: C, 48.24; H, 4.97; N, 10.64%. Anal. for [Fe(2,3,2-3MeO-sal$_2$tet)]ClO_4 (**5**). Calcd for $C_{23}H_{30}N_4O_8ClFe$: C, 47.48; H, 5.20; N, 9.63%. Found: C, 47.42; H, 5.18; N, 9.43%. Anal. for [Fe(2,3,2-mpk$_2$tet)]ClO_4 (**6**). Calcd for $C_{23}H_{30}N_4O_6ClFe$: C, 50.24; H, 5.50; N, 10.19%. Found: C, 49.29; H, 5.56; N, 9.98%. Anal. for [Fe(2,3,2-bpk$_2$tet)]ClO_4 (**7**). Calcd for $C_{33}H_{34}N_4O_6ClFe$: C, 58.81; H, 5.09; N, 8.32%. Found: C, 58.51; H, 5.39; N, 8.08%. Anal. for [Fe(2,2,2-bpk$_2$tet)]-$ClO_4 \cdot EtOH$ (**8**). Calcd for $C_{34}H_{38}N_4O_7ClFe$: C, 57.84; H, 5.43; N, 7.94%. Found: C, 57.48; H, 5.56; N, 7.60%.

Physical Measurements. The magnetic susceptibilities of the polycrystalline samples were measured by the Faraday method using a type 2002 (Cahn Instrument) electrobalance with an electromagnet (0.8 T). Temperatures were controlled over the range 78—298 K by using a digital temperature controller, model 3700 (Scientific Instruments). Variable temperature magnetic susceptibility measurements were carried out. Both heating and cooling rates were controlled manually and magnetic data for one loop were collected in about 10 h. $HgCo(NCS)_4$ was used as a calibration standard. Effective magnetic moments were calculated by use of the formula $\mu_{eff} = (8\chi_m T)^{1/2}$, where χ_m is molar susceptibility after applying a diamagnetic correction.

Mössbauer spectroscopy data were collected by use of a constant-acceleration spectrometer (Austin Science Associates (ASA)). Data were stored in a 1024-channel pulse height analyzer, Type 5200 (Inotech, Inc.). The temperatures were monitored with a calibrated copper vs. constantan thermocouple within a variable-temperature cryostat, Type ASAD-4V-(ASA). A cobalt-57 source of 10 mCi diffused into palladium foil was used for the absorption measurement. Some of the spectra were fitted to the Lorentzian line shape by using a least-squares method at the Computer Center, Kyushu University. Isomer shifts are reported with respect to the centroid of the spectrum of iron foil enriched with ^{57}Fe.

Electronic spectra of a acetonitrile solution containing samples (5×10^{-5} mol dm^{-3}) and reflection spectra were recorded using a UV-3100PC UV-vis-NIR scanning spectrophotometer (Shimadzu) in the region from 300 to 800 nm at 298 K.

Cyclic voltammograms of the complexes were measured in acetonitrile with 0.1 M tetra-*n*-butylammonium perchlorate (1 M = 1 mol dm^{-3}) using a a.c. d.c. Cyclic polarograph P-900 (Yanaco); each measurement was conducted at 298 K under argon atmosphere. The scan rate was 100 m V s^{-1}. A standard three-electrode system was used for cyclic voltammetry experiments comprising a glassy carbon working electrode, a saturated Ag/AgCl reference electrode, and a counter electrode of platinum. Ferrocene was used as a standard substance. The observed values for the complexes were converted to redox potentials versus SCE by using Eq. 1.

Redox potential for a complex (vs. SCE)
=observed value for the complex−observed value for Ferrocene
+0.0739 (Ag/AgCl vs. ferrocene)+0.272 (Ag/AgCl vs. SCE) (1)

Data Collection for X-Ray Crystallography. All measurements were made on a Rigaku AFC7R diffractometer with graphite monochromated Mo K_α radiation and a 12 kW rotating anode generator. The data were collected at room temperature using the ω–2θ scan technique to a maximum 2θ value of 50.0°.

Structure Solution and Refinement. The structures were solved with heavy-atom Patterson methods[13] and expanded using Fourier techniques.[14] The non-hydrogen atoms were refined anisotropically. Hydrogen atoms were included in the calculation but not refined.[15] The weighting scheme was based on counting statistics and included a factor (p=0.001 or 0.01) to down weight the intense reflections. Plots of $\sum w(|F_o|-|F_c|)^2$ versus $|F_o|$, reflection order in data collection, sin θ/λ and various classes of indices showed no unusual trends. Neutral atom scattering factors were taken from Cromer and Waber.[16] Anomalous dispersion effects were included in F_{calcd}.[17]

Results and Discussion

Magnetic Susceptibility. Iron(III) complexes with different anions were prepared to examine the magnetic properties of these iron(III) complexes in addition to those of which the structures were determined by X-ray diffraction. The temperature dependencies of magnetic susceptibilities were measured. The magnetic moments for the representative complexes are collected in Table 1. [Fe(3,3,3)-sal$_2$tet)]NO_3 was in the high-spin state in accordance with a report,[11] and the anion derivatives [Fe(3,3,3)-sal$_2$tet)]X (X=ClO_4^-: 6.07 B.M. (298 K), 6.03 B.M. (78 K), X=PF_6^-: 6.00 B.M. (298 K), 5.97 B.M. (78 K)) were in the same spin state and [Fe(3,3,3)-sal$_2$tet)]BPh_4 in the low-spin state (2.04 B.M. (298 K)). [Fe(3,2,3)-sal$_2$tet)]X (X=NO_3^-, PF_6^-: 1.98 B.M. (298 K) and X=BPh_4^-, [Fe(3,2,3)-mpk$_2$tet)]PF_6 and [Fe(3,2,3)-bpk$_2$tet)]ClO_4: 2.00 B.M. (298 K) were all in the low-spin state. The magnetic moments of [Fe(2,3,2)-sal$_2$tet)]X were as follows: X=NO_3^-: 5.14 B.M. (298 K), 4.91 B.M. (78 K), X=PF_6^-: 5.91 B.M. (298 K), 6.08 B.M. (78 K), and X=BPh_4^-: 5.75 B.M. (298 K), 5.82 B.M. (78 K). The values of the magnetic moments for [Fe(2,3,2)-sal$_2$tet)]NO_3 are abnormal because the complex is a mixture of high-spin and low-spin species, as was confirmed by the measurement of Mössbauer spectra for the complex at 298 and 78 K. It is reported that [Fe(2,2,2)-sal$_2$tet)]$NO_3 \cdot H_2O$ is in the low-spin

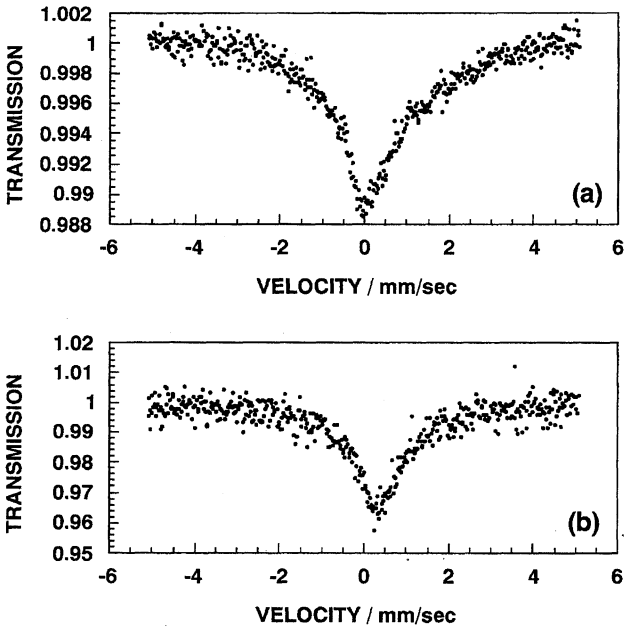

Fig. 1. Mössbauer spectra for (a) [Fe(2,2,2-bpk$_2$tet)]-$ClO_4 \cdot$EtOH (**8**) and (b) [Fe(2,3,2-sal$_2$tet)]ClO_4 (**4**).

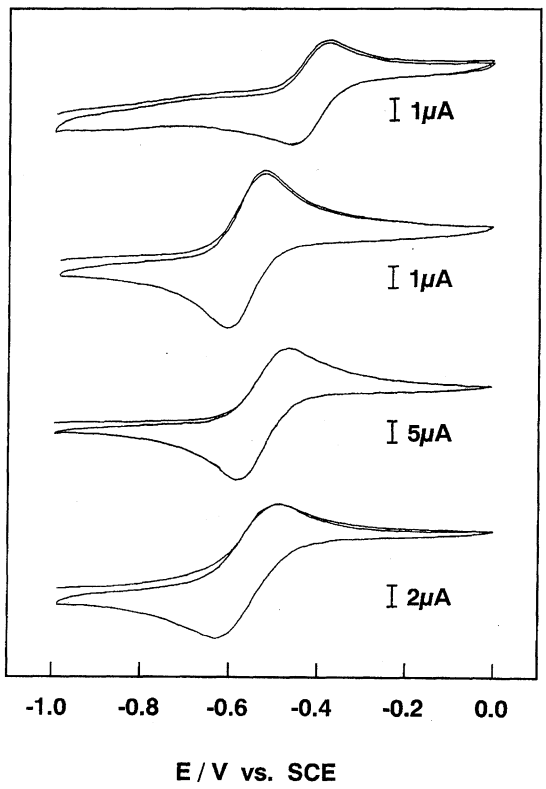

Fig. 2. Cyclic voltammographs for (a) [Fe(3,3,3-sal$_2$tet)]-BPh_4, (b) [Fe(3,2,3-sal$_2$tet)]BPh_4, (c) [Fe(2,3,2-sal$_2$tet)]-BPh_4, and (d) [Fe(2,2,2-sal$_2$tet)]BPh_4.

Table 1. Magnetic Moments, Mössbauer Parameters, Electronic Data and Redox Potentials for the Iron(III) Complexes

Complexes	Magnetic moments[1] (298 K)	(78 K)	Mössbauer parameters[2] δ	ΔE_q	Γ_-	Γ_+	Electronic spectra[3] Ref.[4]	Abs.[4] (ε)[5]	Redox potentials[6]
	μ_{eff}/B.M.		mm s^{-1}		mm s^{-1}		$\times 10^4$ cm^{-1}	($\times 10^3$ l/mol cm)	$E_{1/2}$/V
[Fe(3,2,3-sal$_2$tet)]NO_3 (**1**)	2.03	—[7]	0.17	2.23	0.31	0.34	1.72	1.77 (4.24)	−0.61
[Fe(3,2,3-sal$_2$tet)]BPh_4 (**2**)	1.86	—[7]	0.17	2.16	0.44	0.31	1.67	1.77 (4.56)	−0.61
[Fe(3,2,3-mpk$_2$tet)]PF_6 (**3**)	2.08	—[7]	0.21	2.10	0.84	0.45	1.79	1.87 (4.20)	−0.59
[Fe(2,3,2-sal$_2$tet)]ClO_4 (**4**)	5.96	6.01	0.36	0	1.40		1.82	1.96 (3.15)	−0.53
[Fe(2,3,2-3MeO-sal$_2$tet)]ClO_4 (**5**)	5.95	6.12	0.24	—[8]	1.46	—[8]	1.60	1.79 (3.03)	−0.52
[Fe(2,3,2-mpk$_2$tet)]ClO_4 (**6**)	5.86	5.99	0.37	0.82	1.26	0.94	1.82	2.01 (3.51)	−0.67
[Fe(2,3,2-bpk$_2$tet)]ClO_4 (**7**)	1.91	—[7]	0.17	2.46	0.43	0.40	1.82	1.94 (2.34)	−0.61
[Fe(2,2,2-bpk$_2$tet)]$ClO_4 \cdot$EtOH (**8**)	5.52	5.23	0.18	—[8]	2.06	—[8]	1.80	2.06 (3.08)	−0.65

1) Errors are estimated to be about ±0.06 B.M. 2) Errors are estimated to be about ±0.02 mm s^{-1}. 3) Errors are estimated to be about ±500 cm^{-1} in solid and ±200 cm^{-1} in acetonitrile. 4) Ref: Reflection spectra, Abs: Absorption spectra. 5) ε is molar absorption coefficient. 6) Errors are estimated to be about ±0.01 V. 7) The data are not measured. 8) This value was not calculated because the high-energy peak could not resolved. Therefore the isomer shift value calculated may contain much error.

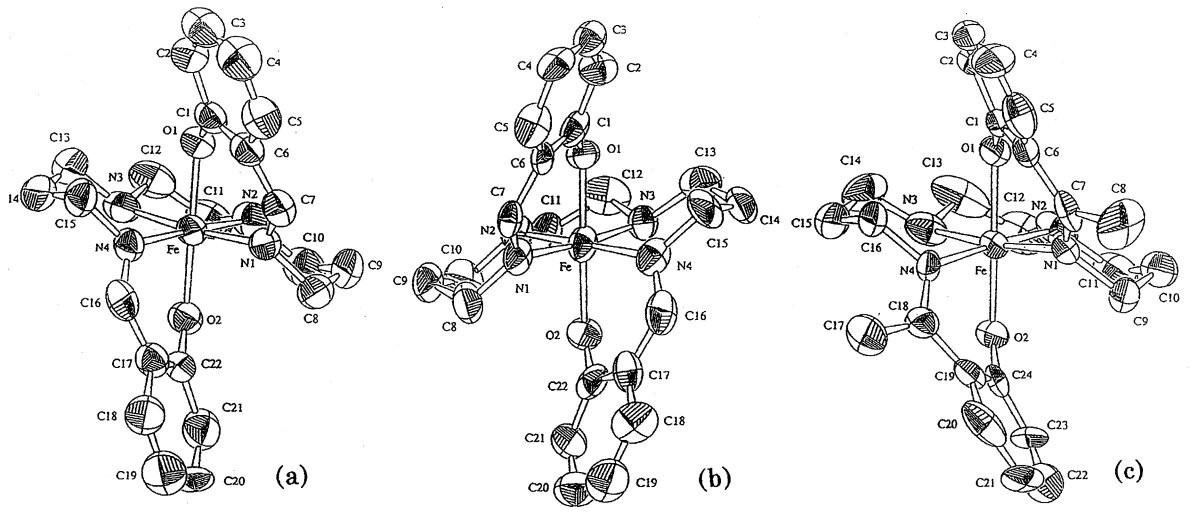

1 **2** **3**

Fig. 3. ORTEP views for the cations of (a) [Fe(3,2,3-sal$_2$tet)]NO_3 (**1**), (b) [Fe(3,2,3-sal$_2$tet)]BPh_4 (**2**), and (c) [Fe(3,2,3-mpk$_2$tet)]PF_6 (**3**).

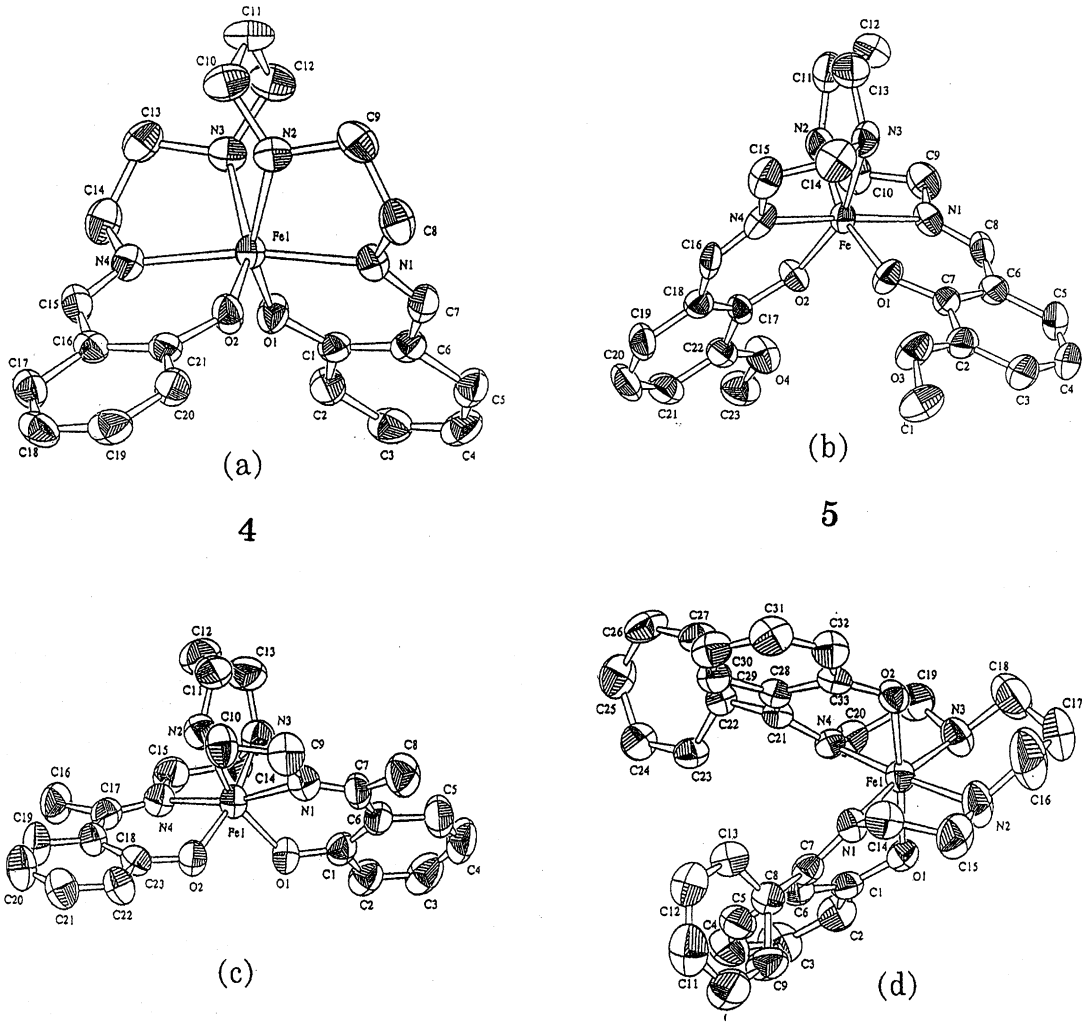

4 **5** **6** **7**

Fig. 4. ORTEP views for the cations of (a) [Fe(2,3,2-sal$_2$tet)]ClO_4 (**4**), (b) [Fe(2,3,2-3OMe-sal$_2$tet)]ClO_4 (**5**), (c) [Fe(2,3,2-mpk$_2$tet)]ClO_4 (**6**), and (d) [Fe(2,3,2-bpk$_2$tet)]ClO_4 (**7**).

Table 2. Crystallographic Data for **1**, **2**, **3**, **4**, **5**, **6**, **7**, and **8**

Complexes	**1**	**2**	**3**	**4**
Empirical formula	$C_{22}H_{28}N_5O_5Fe$	$C_{46}H_{48}N_4O_2BFe$	$C_{24}H_{32}N_4O_2PF_6Fe$	$C_{21}H_{26}N_4O_6ClFe$
Formula weight	498.344	755.57	609.35	521.76
Crystal dimensions/mm	$0.3\times0.3\times0.4$	$0.1\times0.1\times0.2$	$0.2\times0.2\times0.3$	$0.3\times0.3\times0.5$
Crystal system	Monoclinic	Monoclinic	Monoclinic	Orthorhombic
Space group	$P2_1/c$ (#14)	$P2_1/n$ (#14)	$P2_1/c$ (#14)	$Pbcn$ (#60)
a/Å	7.607(1)	14.390(6)	9.37(6)	11.041(2)
b/Å	16.063(1)	20.617(8)	24.15(7)	17.251(2)
c/Å	19.063(1)	14.754(5)	12.85(3)	11.722(2)
α/°	90	90	90	90
β/°	91.00(2)	115.85(2)	97.7(3)	90
γ/°	90	90	90	90
V/Å^3	2329(3)	3939(2)	2880(17)	2232(1)
Z	4	4	4	4
D_{calcd}/g cm^{-3}	1.42	1.27	1.41	1.55
D_{obsd}/g cm^{-3}	1.39	1.25	1.34	1.54
μ(MoK_α)/cm^{-1}	6.90	4.26	6.45	8.41
Radiation (MoK_α)/Å	0.71069	0.71069	0.71069	0.71069
No. of reflection measured	4605	7458	5569	2258
R	0.058	0.063	0.109	0.039
R_w	0.042	0.067	0.136	0.028

Complexes	**5**	**6**	**7**	**8**
Empirical formula	$C_{23}H_{30}N_4O_8ClFe$	$C_{23}H_{30}N_4O_6ClFe$	$C_{33}H_{34}N_4O_6ClFe$	$C_{34}H_{38}N_4O_7ClFe$
Formula weight	581.81	549.81	673.95	706.00
Crystal dimensions/mm	$0.3\times0.3\times0.3$	$0.4\times0.4\times0.6$	$0.4\times0.4\times0.6$	$0.3\times0.4\times0.5$
Crystal system	Orthorhombic	Orthorhombic	Triclinic	Monoclinic
Space group	$Pccn$ (#56)	$Pbca$ (#61)	$P\bar{1}$ (#2)	$P2_1/c$ (#14)
a/Å	14.567(1)	28.249(4)	10.241(3)	14.553(4)
b/Å	22.288(1)	13.989(4)	17.373(1)	14.079(4)
c/Å	15.477(1)	13.174(4)	9.692(7)	16.959(6)
α/°	90	90	105.95(6)	90
β/°	90	90	91.61(4)	94.92(3)
γ/°	90	90	93.83(4)	90
V/Å^3	5025(4)	5205(1)	1652(1)	3461(1)
Z	8	8	2	4
D_{calcd}/g cm^{-3}	1.54	1.40	1.36	1.35
D_{obsd}/g cm^{-3}	1.51	1.43	1.41	1.34
μ(MoK_α)/cm^{-1}	7.62	7.25	5.86	5.64
Radiation (MoK_α)/Å	0.71069	0.71069	0.71069	0.71069
No. of reflection measured	4956	5148	6179	6651
R	0.063	0.082	0.071	0.084
R_w	0.062	0.084	0.076	0.077

state[9] and that [Fe(2,2,2)-sal$_2$tet)]BPh$_4$ shows spin-crossover behavior depending on temperature,[9,12] and the values of the magnetic moments for [Fe(2,2,2-bpk$_2$tet)]ClO$_4$·EtOH are abnormal because the complex is a mixture of high-spin and low-spin species.

Mössbauer Spectra. The Mössbauer spectra of the iron complexes prepared here were measured. The Mössbauer parameters for the representative complexes are collected in Table 1. The spin states expected from the Mössbauer spectra of the complexes agreed with those obtained from the magnetic measurements for the corresponding complexes. The Mössbauer spectrum of **8** at 298 K is shown in Fig. 1(a), which shows an asymmetric absorption (δ=0.18 mm s^{-1}, ΔE_q=0 mm s^{-1}, Γ_-=2.06 mm s^{-1}) and the high energy peak is too broad to be observed. The complex is in high-spin state with ^{6}A and the volume per one molecule is large, 865 Å^3. A longer distance between a iron atom and the neighbor paramagnetic ions (Fe^{3+}) would bring about spin–spin and/or spin–lattice relaxation which are not rapid relative to the ^{57}Fe nuclear Larmor precession frequency. Intermediate paramagnetic relaxation broadens the $|I=1/2, M_\pm=\pm1/2>_g\rightarrow |I=3/2, M_\pm=\pm3/2>_e$ quadrupole component more than the $|I=1/2, M_\pm=\pm1/2>_g\rightarrow|I=3/2, M_\pm=\pm1/2>_e$ component.[18] The observed spectra suggest that the sign of the electric field gradient is positive. Similar asymmetric spectra are observed in **5** and **6**. The Mössbauer spectrum of **4** shows a symmetric broad absorption, as shown in Fig. 1(b). All the low-spin complexes showed a large doublet characteristic of low-spin

Table 3. Representative Bond Distances (Å), Angles (°), the Mean Deviations from the Least-Squares Plane (Å) and the Dihedral Angle between two Phenyl Rings of the Schiff-Base (°) for **1**, **2**, **3**, and **7**

	1	**2**	**3**	**7**
	Bond distances (Å)			
Fe–O(1)	1.876(4)	1.891(8)	1.86(1)	1.886(5)
Fe–O(2)	1.872(4)	1.896(8)	1.87(1)	1.895(5)
Fe–N(1)	1.944(5)	1.95(1)	1.94(1)	1.922(6)
Fe–N(2)	2.021(4)	2.019(9)	2.01(2)	2.017(7)
Fe–N(3)	2.014(5)	2.006(10)	2.02(2)	2.008(6)
Fe–N(4)	1.959(4)	1.958(10)	1.98(2)	1.916(6)
	Bond angles (°)			
O(1)–Fe–O(2)	175.5(2)	174.6(4)	172.1(5)	176.8(3)
O(1)–Fe–N(1)	89.5(2)	91.5(4)	87.7(6)	87.8(3)
O(1)–Fe–N(2)	90.0(2)	89.6(4)	87.7(6)	91.8(3)
O(1)–Fe–N(3)	85.1(2)	84.3(4)	86.6(6)	85.9(3)
O(1)–Fe–N(4)	93.6(2)	92.5(4)	96.2(6)	90.1(3)
O(2)–Fe–N(1)	93.5(2)	93.1(4)	98.2(6)	90.9(3)
O(2)–Fe–N(2)	86.6(2)	87.5(4)	86.9(7)	90.9(3)
O(2)–Fe–N(3)	91.7(2)	90.8(4)	87.1(6)	95.7(3)
O(2)–Fe–N(4)	89.6(2)	90.0(4)	88.7(6)	87.3(3)
N(1)–Fe–N(2)	90.4(2)	89.7(4)	91.9(7)	84.0(3)
N(1)–Fe–N(3)	173.3(2)	172.8(4)	173.4(6)	172.1(3)
N(1)–Fe–N(4)	94.0(2)	95.5(5)	93.3(6)	100.2(3)
N(2)–Fe–N(3)	85.6(2)	84.4(4)	84.5(8)	91.5(3)
N(2)–Fe–N(4)	174.3(2)	174.3(5)	173.6(6)	175.5(3)
N(3)–Fe–N(4)	90.3(2)	90.5(5)	90.7(7)	84.6(3)
The mean deviations from the least-squares plane (Å)				
N(1)–N(2)–N(3)–N(4)	0.0783	0.0565	0.0803	0.0747
O(1)–N(1)–O(2)–N(3)	0.0090	0.0288	0.0094	0.0622
O(1)–N(2)–O(2)–N(4)	0.0117	0.0065	0.0065	0.0479
The dihedral angle between two phenyl rings of the schiff-base (°)				
	49.22	49.39	25.98	155.42

Table 4. Representative Bond Distances (Å), Angles (°), the Mean Deviations from the Least-Squares Plane (Å), and the Dihedral Angle between Two Phenyl Rings of the Schiff-Base (°) for **4**, **5**, **6**, and **8**

	4	**5**	**6**	**8**
	Bond distances (Å)			
Fe–O(1)	1.924(3)	1.924(6)	1.897(5)	1.892(5)
Fe–O(2)	1.924(3)	1.929(5)	1.89(1)	1.867(5)
Fe–N(1)	2.134(3)	2.115(7)	2.123(8)	2.131(6)
Fe–N(2)	2.207(3)	2.222(7)	2.153(9)	2.158(6)
Fe–N(3)	2.207(3)	2.193(8)	2.21(2)	2.152(6)
Fe–N(4)	2.134(3)	2.125(7)	2.122(8)	2.129(6)
	Bond angles (°)			
O(1)–Fe–O(2)	112.7(2)	101.6(3)	96.0(3)	102.3(3)
O(1)–Fe–N(1)	84.4(1)	84.9(3)	84.1(3)	86.4(3)
O(1)–Fe–N(2)	153.8(1)	163.2(3)	161.1(2)	160.6(3)
O(1)–Fe–N(3)	85.8(1)	89.0(3)	87.5(3)	90.9(3)
O(1)–Fe–N(4)	90.3(1)	90.3(3)	105.8(3)	96.7(3)
O(2)–Fe–N(1)	90.3(1)	96.6(3)	100.5(5)	96.0(3)
O(2)–Fe–N(2)	85.8(1)	84.4(3)	90.4(3)	91.8(3)
O(2)–Fe–N(3)	153.8(1)	160.9(3)	162.9(3)	159.7(3)
O(2)–Fe–N(4)	84.4(1)	84.6(3)	86.0(5)	85.6(3)
N(1)–Fe–N(2)	76.9(1)	78.8(3)	77.2(3)	78.1(3)
N(1)–Fe–N(3)	110.6(1)	100.1(3)	96.6(4)	100.2(3)
N(1)–Fe–N(4)	170.3(2)	175.2(3)	167.7(2)	176.1(3)
N(2)–Fe–N(3)	83.8(2)	89.9(3)	91.5(3)	79.7(3)
N(2)–Fe–N(4)	110.6(1)	106.0(3)	92.4(3)	98.4(3)
N(3)–Fe–N(4)	76.9(1)	79.5(3)	76.9(4)	77.5(3)
The mean deviations from the least-squares plane (Å)				
O(1)–N(1)–N(2)–N(4)	0.2143	0.6702	0.0272	0.0934
O(1)–O(2)–N(2)–N(3)	0.3880	0.3038	0.3133	0.2876
O(2)–N(1)–N(3)–N(4)	0.2143	0.7289	0.0925	0.0708
The dihedral angle between two phenyl rings of the schiff-base (°)				
	108.43	97.32	59.31	45.63

complexes.

Electronic Spectra. Wilson et al.[6,10] have reported that [Fe(2,2,2)-sal$_2$tet)]X shows spin-crossover behavior in distilled water, and that an absorption band at 16700 cm^{-1} is assigned to the LMCT transition of low-spin species and an absorption band at 20000 cm^{-1} is assigned to the LMCT transition of the high-spin species. The absorptions for [Fe(2,2,2)-sal$_2$tet)]PF_6 and [Fe(2,2,2)-sal$_2$tet)]$NO_3\cdot H_2O$ in distilled water were analyzed as a superposition of them. Absorption spectra for [Fe(3,3,3-sal$_2$tet)]NO_3 and [Fe(3,2,3-sal$_2$tet)]NO_3 in methanol were analyzed by Ito et al. under the assumption that the spectra are composed of a superposition of an absorption at 16700 cm^{-1} and one at 20000 cm^{-1}.[11]

Electronic spectra for the iron(III) complexes with the hexadentate ligands prepared here were measured in solid state and in acetonitrile at 298 K. Absorption bands at 14000—25000 cm^{-1} with the absorption coefficients are collected in Table 1. The UV-visible data for the complexes prepared here are similar to those described above. The LMCT bands for the low-spin complexes seem to be about 10^3 cm^{-1} smaller than those for the high-spin complexes. The absorption bands in acetonitrile are about 500—2600 cm^{-1} blue shifted compared with those of the corresponding reflection spectra. The blue shift of 2600 cm^{-1} observed in acetonitrile compared with the absorption band in solid state for [Fe(2,2,2-bpk$_2$tet)]$ClO_4\cdot$EtOH is due to the appearance of low-spin species.

Cyclic Voltammetry. The redox potentials were measured for the iron(III) complexes. The representative voltammographs are shown in Fig. 2. The quasi-reversible waves due to Fe^{2+}–Fe^{3+} redox were observed from −0.52 to −0.67 V. The data are collected in Table 1, in which the values listed show that the redox values are greatly influenced by a methyl or a phenyl substitution of the ligands. The average values observed for the complexes without a methyl or phenyl substitution were −0.45±0.01 V for [Fe(3,3,3-sal$_2$tet)]-X, −0.61±0.01 V for [Fe(3,2,3-sal$_2$tet)]X, −0.53±0.01 V for [Fe(2,3,2-sal$_2$tet)]X and −0.59±0.01 V for [Fe(2,2,2-

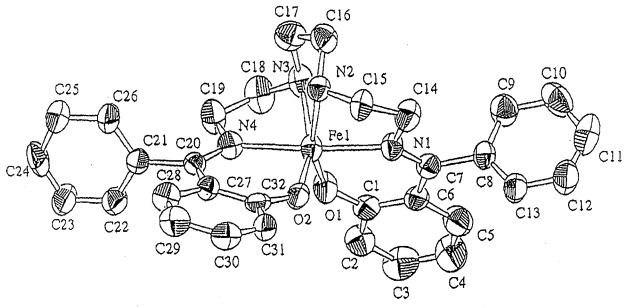

8

Fig. 5. ORTEP view for the cation of [Fe(2,2,2-bpk$_2$tet)]-ClO_4·EtOH (**8**).

sal$_2$tet)]X (X=NO_3^-, ClO_4^-, PF_6^-, BPh_4^-, and Cl^-).[19] There are some factors affecting the redox potentials of complexes, for example: i) negative charge of ligands, ii) σ donor strength of the ligands, iii) π acceptor strength of the ligands, iv) variation of spin states, and v) steric factors. The observed data show that the average redox potentials for [Fe(3,2,3-sal$_2$tet)]X (low-spin species) are shifted about 0.01—0.16 V to a negative potential relative to those for the other complexes. If it is supposed that the above factors i), ii), and iii) are identical for the 3,3,3, 3,2,3, 2,3,2, and 2,2,2 systems, and that the differences in steric factor between the 2,2,2 and 2,3,2 system, between the 2,3,2 and 3,2,3 system, and between the 3,2,3 and 3,3,3 system are identical, the potential value of "[Fe(3,2,3-sal$_2$tet)]$^+$ in high-spin state" is supposed to be -0.49 V. Accordingly, the difference in redox potential between high-spin and low-spin states is calculated to be 0.12 V; the potential value of the low-spin state must be more negative than that of the high-spin state.

[Fe(3,3,3-sal$_2$tet)]NO_3 and [Fe(2,2,2-sal$_2$tet)]X (X=NO_3^- and PF_6^-)[6,10] are in spin-crossover state in acetonitrile at 298 K, but the potential curves show a single potential instead of a superposition of the potentials of high-spin species and that of low-spin species. This fact may suggest that the electronic state of these complexes in the 3,3,3, 2,3,2, and 2,2,2 systems may be in high-spin state at the time when a redox reaction at a electrode proceeds, although there is a report which says that it is difficult to distinguish the closed peaks.[20] Thus this discussion should be confirmed in future on the base of better data.

Structures of the Compounds. The ORTEP views of the complexes **1**, **2**, and **3** with the 3,2,3 system shown are in Figs. 3(a), 3(b), and 3(c), respectively, the crystallographic data are given in Table 2, and the final positional parameters of the atoms are given in supplemental materials. The bond distances and bond angles of these complexes, and the mean deviations for least-squares plane formed by the coordination atoms of these complexes are collected in Table 3. These three complexes have the same space group (#14), and the bond distances of Fe–N (or O) are similar to each other. The iron atoms of the complexes are in the center of an approximately octahedral geometry, with two oxygen atoms *trans* to each other and imino nitrogen atoms *cis*; this moiety is called *trans*-FeN_4O_2 here. The values of bond distances Fe–O, Fe–N_{imine}, and Fe–N_{amine} observed for the three complexes are characteristic of those of low-spin complexes.[9,11,12] The average bond angles of O(1)–Fe–O(2), N(1)–Fe–N(3), and N(2)–Fe–N(4) for **1**, **2**, and **3** are 174.1°, 173.2°, and 174.1°, all larger than 168.3° for [Fe(3,3,3-sal$_2$tet)]NO_3.[11] These complexes are low-spin complexes with *trans* geometry and [Fe(3,3,3-sal$_2$tet)]NO_3[11] is a high-spin complex with the same geometry. The *trans*-FeN_4O_2 core of the 3,3,3-sal$_2$tet coordination system is somewhat distorted from octahedral geometry, in contrast to the 3,2,3-sal$_2$tet system, which suggests that a moiety around an iron atom of the 3,3,3-sal$_2$tet system is sterically crowed compared to that of the 3,2,3-sal$_2$tet system. The average deviations from least-squares planes formed by N(1)–N(2)–N(3)–N(4), O(1)–N(1)–O(2)–N(3), and O(1)–N(2)–O(2)–N(4) for **1** is 0.033 Å and the average deviation of an iron atom from these planes is 0.042 Å, and those for the other complexes are similar to each other. Almost no effect due to the substitution by a methyl group instead of a hydrogen on the steric geometry is observed, except that the difference in the bond lengths of Fe–N_{imine} for **3** is a little larger than that for **1**or **2**.

The structure of **1** has been before reported by Ito et al.[11] and is a δ type for two nitrogen atoms (N(2) and N(3)) and two carbon atoms (C(11) and C(12)) of the 3,2,3-tetramine moieties.[21] On the other hand, the structure of a crystal solved here is a λ type. The bond distances and bond angles of the complexes are the same as the corresponding value of the crystal with a δ type within the experimental errors. The complex ion and a nitrate ion are held together by a N(3)–H(17)···O(3) hydrogen bond with the bond length of 2.34(5) Å.

The ORTEP views of the complexes **4**, **5**, **6** and **7** with the 2,3,2-system are shown in Figs. 4(a), 4(b), 4(c), and 4(d), the crystallographic data are given in Table 2, and the final positional parameters for the atoms are given in the supplemental materials. The bond distances and bond angles for **4**, **5**, and **6** are collected in Table 4 with the data for **8**, and those of **7** are collected in Table 3. The high-spin complexes **4**, **5**, and **6** have similar space groups and a *cis*-FeN_4O_2 geometry. The values of the bond distances Fe–O, Fe–N_{imine}, and Fe–N_{amine} are characteristic of high-spin iron(III) complexes.[22—30] The values of the bond angles O(1)–Fe–N(2), N(1)–Fe–N(4), and O(2)–Fe–N(3) suggest that the FeN_4O_2 geometry is very distorted from a regular octahedron. The mean deviations for the least-squares planes formed by O(1)–N(1)–N(2)–N(4), O(1)–O(2)–N(2)–N(3), and O(2)–N(1)–N(3)–N(4) are larger than those for the complexes with the 3,2,3-system, and the mean deviation of an iron atom from these planes is 0.184 Å for **4**. The Mössbauer spectrum of **4** shows a broad symmetric absorption (Fig. 1(b)); δ=0.361 mm s^{-1}, ΔE_q=0 mm s^{-1}, and Γ=1.397 mm s^{-1}. The distortion of the FeN_4O_2 geometry suggests that the efg of an iron atom exists as the first approximation. Therefore the electrostatic contribution of the charges of other ions in the solid to the efg would cancel the efg and bring about ΔE_q=0.

On the other hand, the geometry of the iron atoms of **7** is *trans*-FeN_4O_2. The average bond distances Fe–O, Fe–N_{imine},

and Fe–N_{amine} are 1.891, 1.920, and 2.013 Å, respectively. The average bond angle of O(1)–Fe–O(2), N(1)–Fe–N(3), and N(2)–Fe–N(4) is 174.8°, which is similar to those of **1**, **2**, and **3** with *trans*-FeN_4O_2 geometry. The complex **6** with 2,3,2-mpk$_2$tet is in the high-spin state with *cis*-FeN_4O_2 and the complex **7** with 2,3,2-bpk$_2$tet is in the low-spin state with *trans*-FeN_4O_2. The substituting of a phenyl group instead of a hydrogen brings about the changes in the geometry and magnetic properties (electronic ground state).

The ORTEP view of **8** is shown in Fig. 5 and the crystallographic data are given in Table 2. The moiety of an iron atom is *cis*-FeN_4O_2 geometry. The mean deviations for the least-squares planes are larger than those of [Fe(2,2,2-sal$_2$tet)]-NO_3·H_2O in the low-spin state with *cis*-FeN_4O_2 geometry.[9] The deviations of an iron atom from these planes are similar to the corresponding values of [Fe(2,2,2-sal$_2$tet)]BPh_4 which is in high-spin state at room temperature.[12] There are hydrogen bonds between an ethanol molecule and the complex ion, the complex ion and a perchlorate ion, and the ethanol molecule and the perchlorate ion: O(7)–H(38)···N(3), N(2)–H(31)···O(3), and O(7)–H(38)···O(4). Their hydrogen bond distances are 2.32, 2.16, and 2.66 Å, respectively.

Conclusions

The ligand field strength of the ligands of the iron(III) complexes [Fe(3,3,3-sal$_2$tet)]X, [Fe(3,2,3-sal$_2$tet)]X, [Fe(2,3,2-sal$_2$tet)]X, [Fe(2,2,2-sal$_2$tet)]X (X=NO_3^-, ClO_4^-, PF_6^-, BPh_4^-, and Cl^-) and those of their derivatives lie close a spin-crossover point in the electronic ground state. The average bond lengths of Fe–O, Fe–N_{imine}, and Fe–N_{amine} for the four high-spin complexes examined here are 1.906±0.022, 2.126±0.007, and 2.188±0.029 Å, respectively, and the average values for the four low-spin complexes examined here are 1.881±0.013, 1.945±0.021, and 2.014±0.006 Å, respectively. The average Fe–O bond distance for the high-spin complexes is slightly longer (0.025 Å) than that for the low-spin complexes. The average Fe–N_{imine} and Fe–N_{amine} bond distances in the high-spin complexes are 0.181 and 0.171 Å longer than the corresponding values in the low-spin complexes. The bond angles of the three axials L–Fe–L′ (*trans* position) are considerably deviated from 180° in the high-spin complexes, and close to 180° in the low-spin complexes. The mean deviations of the least-squares planes formed by the coordination atoms of the high-spin complexes are larger than those of the low-spin complexes. The average mean deviations for the least-squares planes formed by N(1)–N(2)–N(3)–N(4), O(1)–N(1)–O(2)–N(3), and O(1)–N(2)–O(2)–N(4) of the low-spin complexes are 0.072±0.011, 0.027±0.025, and 0.018±0.020 Å, respectively. On the other hand, the average mean deviations for the least-squares planes formed by O(1)–N(1)–N(2)–N(4), O(1)–O(2)–N(2)–N(3), and O(2)–N(1)–N(3)–N(4) of the high-spin complexes are 0.251±0.290, 0.323±0.045, and 0.277±0.308 Å, respectively. The chelate ring for the complexes in the low-spin state is more planar than that in the high-spin state.

In solution, [Fe(3,3,3-sal$_2$tet)]NO_3[11] and [Fe(2,2,2-sal$_2$tet)]X (X=NO_3^- and PF_6^-)[6,10] show spin-crossover behavior depending on temperature. It is confirmed that in solution, [Fe(3,2,3-sal$_2$tet)]NO_3[11] is in the low-spin state and [Fe(2,3,2-sal$_2$tet)]ClO_4 in the high-spin state in our laboratory. In solution, 3,2,3-sal$_2$tet is stronger in the ligand field strength than 3,3,3-sal$_2$tet, and 2,2,2-sal$_2$tet is stronger in the ligand field strength than 2,3,2-sal$_2$tet. These observations show that the length of a methylene chain of the middle chelate ring of three chelate rings formed in a molecule is important; if the middle chelate ring is a five-membered chelate ring, the ligand field becomes strong, which suggests that the conjugation of π electrons from the both sides of the chelate decreases in the system of a six-membered chelate ring. The whole conjugation system of a ligand would be as important as the conjugation systems of individual chelate rings formed by coordination to a metal.

Supplementary Material Available

Complete atomic coordinates, thermal parameters, bond lengths, and angles have been deposited as Document No. 70046 at the Office of the Editor of Bull. Chem. Soc. Jpn. The final positional parameters for the atoms are given in Tables I-1, II-1, III-1, IV-1, V-1, VI-1, VII-1, and VIII-1, the anisotropic displacement parameters in Tables I-2, II-2, III-2, IV-2, V-2, VI-2, VII-2, and VIII-2, the bond distances in Tables I-3, II-3, III-3, IV-3, V-3, VI-3, VII-3, and VIII-3, and bond angles in Tables I-4, II-4, III-4, IV-4, V-4, VI-4, VII-4, and VIII-4 for **1**, **2**, **3**, **4**, **5**, **6**, **7**, and **8**, respectively.

References

1) Y. Maeda and Y. Takashima, *Comments Inorg. Chem.*, **7**, 44 (1988).
2) T. Kambara, *J. Chem. Phys.*, **70**, 4199 (1979).
3) T. Kambara, *J. Chem. Phys.*, **74**, 4557 (1981).
4) A. J. Conti, R. K. Chadha, K. M. Sena, A. L. Rheingold, and D. N. Hendrickson, *Inorg. Chem.*, **32**, 2670 (1993).
5) S. Hayami and Y. Maeda. *Inorg. Chim. Acta*, **255**, 181 (1997).
6) M. F. Tweedle and L. J. Wilson, *J. Am. Chem. Soc.*, **98**, 4824 (1976).
7) E. V. Dose, K. M. M. Murphy, and L. J. Wilson, *Inorg. Chem.*, **15**, 2622 (1976).
8) E. V. Dose, M. A. Hoselton, N. Sutin, M. F. Tweedle, and L. J. Wilson, *J. Am. Chem. Soc.*, **100**, 1141 (1978).
9) E. Sinn, G. Sim, E. V. Dose, M. F. Tweedle, and L. J. Wilson, *J. Am. Chem. Soc.*, **100**, 3375 (1978).
10) R. A. Binstead, J. K. Beattie, T. G. Dewey, and D. H. Turner, *J. Am. Chem. Soc.*, **102**, 6442 (1980).
11) T. Ito, M. Sugimoto, H. Ito, K. Toriumi, H. Nakayama, W. Mori, and M. Sekizaki, *Chem. Lett.*, **1983**, 121.
12) Y. Nishida K. Kino, and S. Kida, *J. Chem. Soc., Dalton Trans.*, **1983**, 1957.
13) "SAPI91," Fan Hai-Fu (1991). "Structure Analysis Programs with Intelligent Control," Rigaku Corporation, Tokyo, Japan.
14) "DIRDIF92," P. T. Beurskens, G. Admiraal, G. Beurskens, W. P. Bosman, S. Garcia-Granda, R. O. Gould, J. M. M. Smits, and C. Smykalla, The DIRDIF Program System, Technical Report of the Crystallography Laboratory, University of Nijmegen, The Netherlands, (1992).

15) Least-Squares: Function minimized: $\sum w(|F_o| - |F_c|)^2$ where $w = 1/\sigma^2(F_o) = 4F_o^2/\sigma^2(F_o^2)$, $\sigma^2(F_o^2) = S^2(C+R^2B)+pF_o^2)^2/L_p^2$, S=Scan rate, C=Total Integrated Peak Count, R=Ratio of Scan Time to background counting time, B=Total Background Count, L_p=Lorentz-polarization factor, and p=p-factor.

16) D. T. Cromer and J. T. Waber, "International Tables for X-Ray Crystallography," The Kynoch Press, Birmingham, England (1974), Vol. IV, Table 2.2A.

17) J. A. Ibers and W. C. Hamilton, *Acta Crystallogr.*, **17**, 781 (1964).

18) M. Blume, *Phys. Rev. Lett.*, **18**, 305 (1967).

19) S. Hayami, PH. D. Thesis, "Study of the Structures and Magnetic Behavior of Iron(III) Complexes with Hexadentate Schiff-Base Ligands: in Connection with Spin-Crossover Behavior," Kyushu Univ., 1997.

20) R. L. Myers and I. Shain, *Anal. Chem.*, **41**, No. 7 (1969).

21) B. D. Sarma and J. C. Bailar, Jr., *J. Am. Chem. Soc.*, **77**, 5476 (1995).

22) J. G. Leipoldt and P. Coppens, *Inorg. Chem.*, **12**, 2269 (1973).

23) A. P. Summerton, A. A. Diamantis, and M. R. Snow, *Inorg. Chim. Acta*, **27**, 123 (1978).

24) W. R. Scheidt, D. K. Geiger, and K. J. Haller, *J. Am. Chem. Soc.*, **104**, 495 (1982).

25) M. D. Timken, D. N. Hendrickson, and E. Sinn, *Inorg. Chem.*, **24**, 3947 (1985).

26) N. Matsumoto, S. Ohta, C. Yoshimura, A. Ohyoshi, S. Kohata, H. Okawa, and Y. Maeda, *J. Chem. Soc., Dalton Trans.*, **1985**, 2575.

27) M. D. Timken, C. E. Strouse, S. M. Soltis, S. A. Daverio, D. N. Hendrickson, A. M. Abdel-Mawgoud, and S. R. Wilson, *J. Am. Chem. Soc.*, **108**, 395 (1986).

28) Y. Maeda, H. Oshio, Y. Takashima, M. Mikuriya, and M. Hidaka, *Inorg. Chem.*, **25**, 2958 (1986).

29) B. J. Kennedy, A. C. McGrath, K. S. Murray, B. W. Skelton, and A. H. White, *Inorg. Chem.*, **26**, 483 (1987).

30) H. Oshio, K. Toriumi, Y. Maeda, and Y. Takashima, *Inorg. Chem.*, **30**, 4252 (1991).